

Fig. 1. (Top) Design of DORIS with the decoupled user workspace. The end effector (handle) can be moved freely within the decoupling mechanism, which is disjointed from all the translation links, rotation links, and actuators. The inset figure represents a user manipulating the end effector of DORIS. (Bottom) Design of the decoupling mechanism. Four encoders at each corner are utilized for calculation of the position and angle of the end effector. When the brakes are engaged, the movement of the end effector is no longer allowed. Note that a handle is removed in the top figure to make the structure more clearly visible.

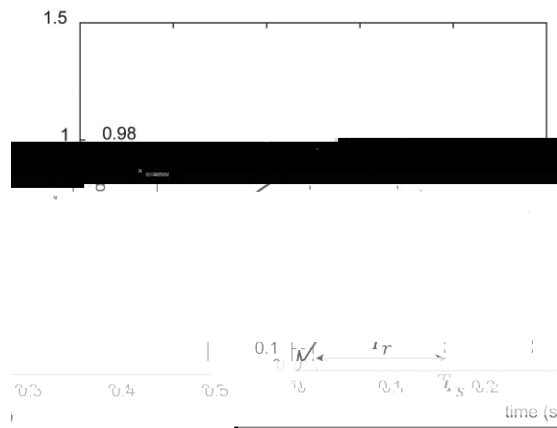
TABLE I
SPECIFICATIONS OF DORIS. ALL ARE MEASURED VALUES

It

Fig. 3. Schematic of the five-bar linkage mechanism inside of the decoupling mechanism. The relative position ($\zeta_{EE/DM}$) and relative rotation angle ($\theta_{EE/DM}$) of the end effector (solid black square) referenced to the decoupling mechanism can be obtained by using four measured angles ($\theta_1, \theta_2, \theta_3$, and

TABLE II

MEASURED MASS



Detailed description of the haptic robot's components and assembly process, including the use of a flat-plate pedal and plasma-assisted technology.

m m

21. B. B. et al., A. et al., C. et al., *Robotics*, vol. 7, no. 2, pp. 15, 2018.
22. D. et al., M. et al., D. et al., *Am. J. Neurosci. Methods*, vol. 181, no. 2, pp. 199–211, Oct. 30, 2009.
23. Z. et al., D. et al., *Int. J. Adv. Robotic Syst.*, vol. 10, no. 10, 2013, Art. ID. 374.
24. E. et al., E. et al., *Mechatronics*, vol. 51, pp. 19–30, 2018.
25. A. et al., A. et al., *Am. J. Neurosci. Methods*, vol. 181, no. 2, pp. 199–211, Oct. 30, 2009.